

Two-Stage Formation Model and Helicity of Gold Nanowires

Yusuke Iguchi,¹ Takeo Hoshi,^{1,2*} Takeo Fujiwara^{1,2†}

¹Department of Applied Physics, The University of Tokyo,
Bunkyo-ku, Tokyo, 113-8656, Japan

²Core Research for Evolutional Science and Technology,
Japan Science and Technology Agency (CREST-JST), Japan

*Present address : Department of Applied Mathematics and Physics,
Tottori University, Tottori 680-8550, Japan

†To whom correspondence should be addressed; E-mail: fujiwara@coral.t.u-tokyo.ac.jp.

A model for the formation of helical multishell gold nanowires is proposed and is confirmed with the quantum mechanical molecular dynamics simulations. The model can explain the magic number of the helical gold nanowires in the multishell structure. The reconstruction from ideal non-helical to realistic helical nanowires consists of two stages: dissociations of atoms on the outermost shell from atoms on the inner shell and slip deformations of atom rows generating (111) structure on the outermost shell. The elementary processes are governed by a competition between *s*- and *d*-electrons together with the width of the *d*-band. The possibility for the helical nanowires of platinum, silver and copper is discussed.

Gold nanowires synthesized by electron beam techniques have helical multishell structures along the [110] direction. (1, 2) The outermost shell consists of the (111) atomic sheets. The

histogram of the appearance of the wire diameters shows peaks of the numbers of atoms discretely at seven, eleven, thirteen, fourteen and so on. The difference of numbers of atoms on the outermost shell and that on the next outermost one is seven, called “magic number”, except cases of five and seven atoms on the outermost shell. Platinum nanowires have the same type of helicity, (3) and, therefore, the helical multishell structure is generic for metals of a certain class. Both classical and quantum mechanical molecular dynamics (MD) simulation studies and the first principles electronic structure calculations have been achieved and the stability and string tension were studied. (4, 5, 6, 7, 8) But no systematic explanation has been given on the formation of the helical nanowire with the magic number.

Here, we propose a two-stage model of formation of multishell helical nanowires, the helicity and the magic number. In the ideal (110) fcc nanowire of stacking (110) sections, there are atom rows parallel to the [110] axis, and we see the multishell structure with no helicity. In Fig. 1(a), three structures of the ideal fcc (110) nanowires, 6-1, 10-4, and 12-6, are shown, where the index stands for the number of atoms on the lateral atom row on the outermost shell, that on the next and so on. The structure of these ideal model nanowires satisfies two conditions: (a) there is no acute angle on the surface, and (b) there is no (001) face with a side longer than that of any (111) face. The condition (a) originates from requirement of diminishing surface tension, and (b) from that of shortening the (001) side length since the surface energy of a (001) surface is higher than that of (111).

The outermost shell should be transformed into a (111) sheet. There are (001) faces on the outermost shell of ideal nanowires and slips of atom rows are necessary to diminish the (001) faces into (111) faces. Before slip of an atom row, the outermost shell should be separated from the inner shell to move freely and atom rows along (110) might be inserted into the outermost shell (Stage 1). When we put one atom row, the distance between atoms on the outermost shell and the center is longer than the nearest neighbor distance. Therefore, in case that the inter-

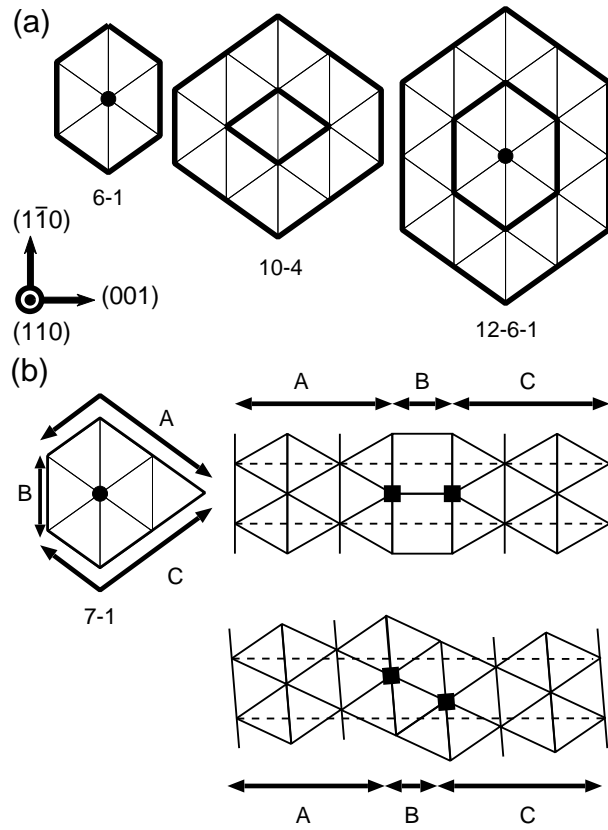


Figure 1: (a) An ideal (110) fcc nanowires is of intrinsic multishell. (b) Expanded sheet of a 7-1 multishell nanowire before (upper right) and after (lower right) surface reconstruction. Dashed lines connect the same atoms at the right and the left ends. Slip in B region transforms a (100) face into a (111) like face, and introduces the helicity on the surface.

atomic interaction on a (111) sheet is dominant for stabilization, one atom row is inserted and the outermost shell can move freely from the inner shell. Then atom rows slip on the outermost shell and the (001) face transforms into (111) (Stage 2).

The outermost shell has six more “bonds” on the lateral row than the inner shell in 6-1, 10-4 1nd 12-6-1 nanowires as shown by bold lines in Fig. 1(a). Then 7-1, 11-4, and 13-6-1 multishell nanowires are formed, by adding one atom row to the outermost shell, as in Fig. 1(b) and the initial states in Figs. 2(a)(b)(d). The outermost shell has seven more atoms on a lateral atom row than the inner shell. This is the origin of the “magic number”. When the number of atoms on the lateral row in the outermost shell is odd, the surface reconstruction brings the helicity to nanowires inevitably as in Fig. 1(b). Helical nanowires of 7-1, 11-4, 14-7-1 and 15-8-1 are experimentally observed. (1)

We performed, to verify the present model, MD simulations of gold nanowires by using tight-binging (TB) Hamiltonian. (9, 10, 11, 12) We stack ideal (110) sections of the fcc lattice, as an initial state, as shown in Fig. 2, nine layers in the cases of 7-1 and 11-4, seven layers in the cases of 12-6-1 and 13-6-1, and six layers in the cases of 14-7-1, and 15-8-1. Then the numbers of atoms are from 76 to 156. Each center of gravity of the both end layers of the nanowires is fixed and no external force is imposed. One MD step corresponds to 1 fs. Figure 2 shows the time evolution of typical sections of gold nanowires. The surface reconstruction is always observed, when an [110] atom row is added as Figs. 2(a), (b), (d)-(f). No significant difference is observed at two different temperatures, 600 K and 900 K, except the case of 12-6-1 nanowire (Fig. 2(c)), where no surface reconstruction is observed at 600 K.

A typical time evolution of MD simulations is shown in Fig. 3 for the 11-4 nanowire (Fig. 2(b)) at 600 K. See also the supplementary movie. The atom A in Fig. 3, which is on the (111) face and also the nearest neighbor of atoms on the (100) face (e.g. the atom B), dissociates from the inner shell before the first 500 MD step (Stage 1). Then, the surface atoms can

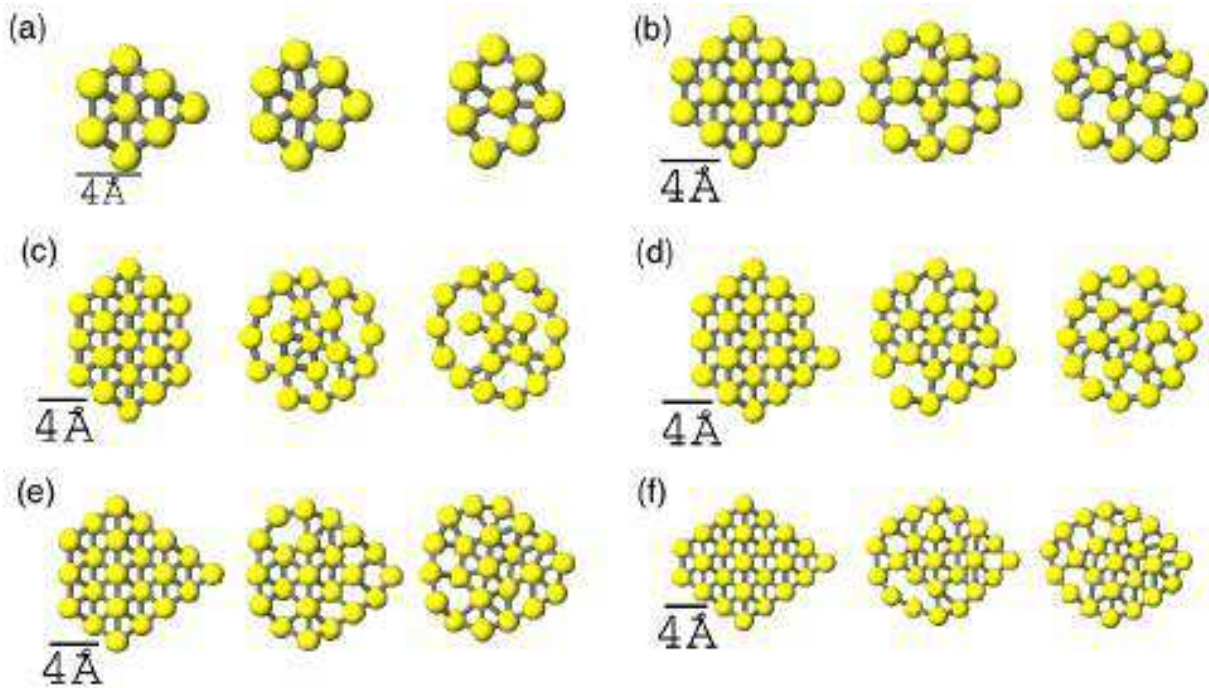


Figure 2: The changes in the sections of gold nanowires: (a) 7-1 at initial state (left), 400 MD step (middle) and 5,000 MD step (right), (b) 11-4 at initial state (left), 400 MD step (middle) and 6,000 MD step (right), (c) 12-6-1 at initial state (left), 7,500 MD step (middle) and 13,000 MD step (right), (d) 13-6-1, at initial state (left), 750 MD step (middle) and 9,000 MD step (right), (e) 14-7-1, at initial state (left), 400 MD step (middle) and 7,000 MD step (right), and (f) 15-8-1 at initial state (left), 400 MD step (middle) and 5,000 MD step (right). There are the reconstruction of the outermost shell sheet in all the nanowires in the figure, and they become helical multishell nanowires. Temperatures in the simulations are 600 K in (a), (b), (e), and (f) and 900 K in (c) and (d).

move almost independently from inner shell. The total energy decreases almost monotonically after the initial 1,000 MD step. During the interval between about 2,000 MD step and 5,000 MD step, a (001) face reconstructs into a hexagonal (111)-like face by the slip deformation, and the helical structure appears (Stage 2). The inner shell rotates at the same time. These behaviors with two stages agree with the present model. It should be noticed that the time evolution in the MD simulation does not totally correspond to a real formation process of gold nanowires. But we believe that the real formation process have two different elementary processes of Stage 1 (short time process) and Stage 2 (long time process).

We study the change of the electronic structures during the surface reconstruction with the slip of an atom row and the introduction of the helicity. Figure 4(a) shows the local electronic density of states (LDOS) of the atom A on (111) area in Stage 1, by using the local coordinate system (around the atom A) that the x axis is the nanowire axis [110] and the y axis is lateral [112]. The local energy of s -orbital increases because of reduction of its coordination number (Fig. 4(a) top). The local energy of yz -orbital increases since the orbital extents perpendicularly to the wire surface and the neighbor distance increases along this direction (not shown). The local energy of xy -orbital decreases (Fig. 4(a) middle). Then the energy loss and gain of the d -orbitals almost cancel with each other and the net change of the local energy of the atom A is mainly due to that of the s -orbital (Fig. 4(a) bottom). In Fig. 4 (b), we present LDOS of the atom C, on the edge of two (111) faces, in Stage 1, by using the local coordinate system that the x axis is the nanowire axis [110] and the y axis is lateral [001]. The local energy of xy -orbital decreases (Fig. 4(b) middle) and those of other d -orbitals are either negative or positive but relatively small (not shown). Therefore, the local energy of the d -orbitals totally decreases on the atom C. We can attribute this energy decrease of d orbitals to the flattened surface around the atom C after the dissociation of the atom A.

After all, actual dissociation is governed by the competition between the s -orbital energy

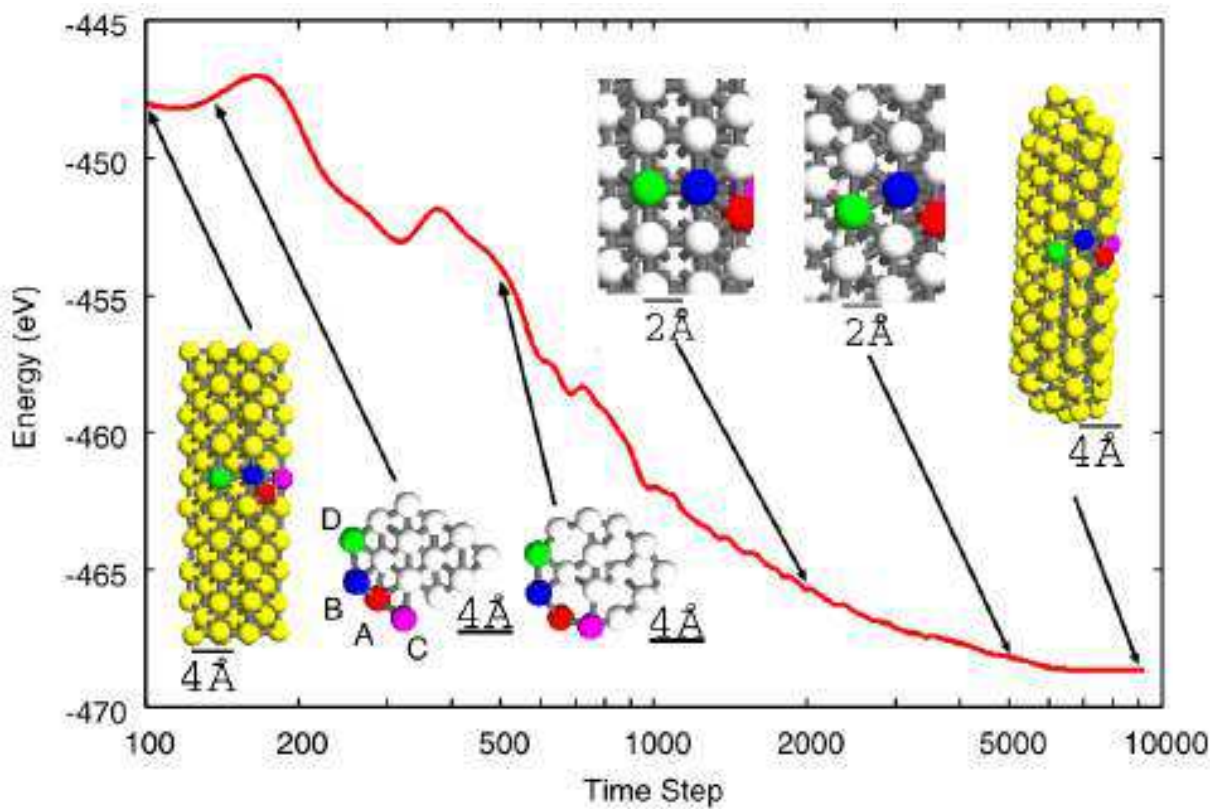


Figure 3: Temperature driven MD development of the total energy and the atomic configuration of the 11-4 nanowire at 600 K. Notice that the MD steps of the horizontal axis is in the logarithmic scale and one MD step is 1 fs. Red, blue, purple, and green atoms are named A, B, C, and D respectively. Within 500 MD step, the atom A was disassociated from inner shell. Between 2,000 and 5,000 MD step, the slip between the atom B and D brought the surface reconstruction, and (001) face becomes (111) face.

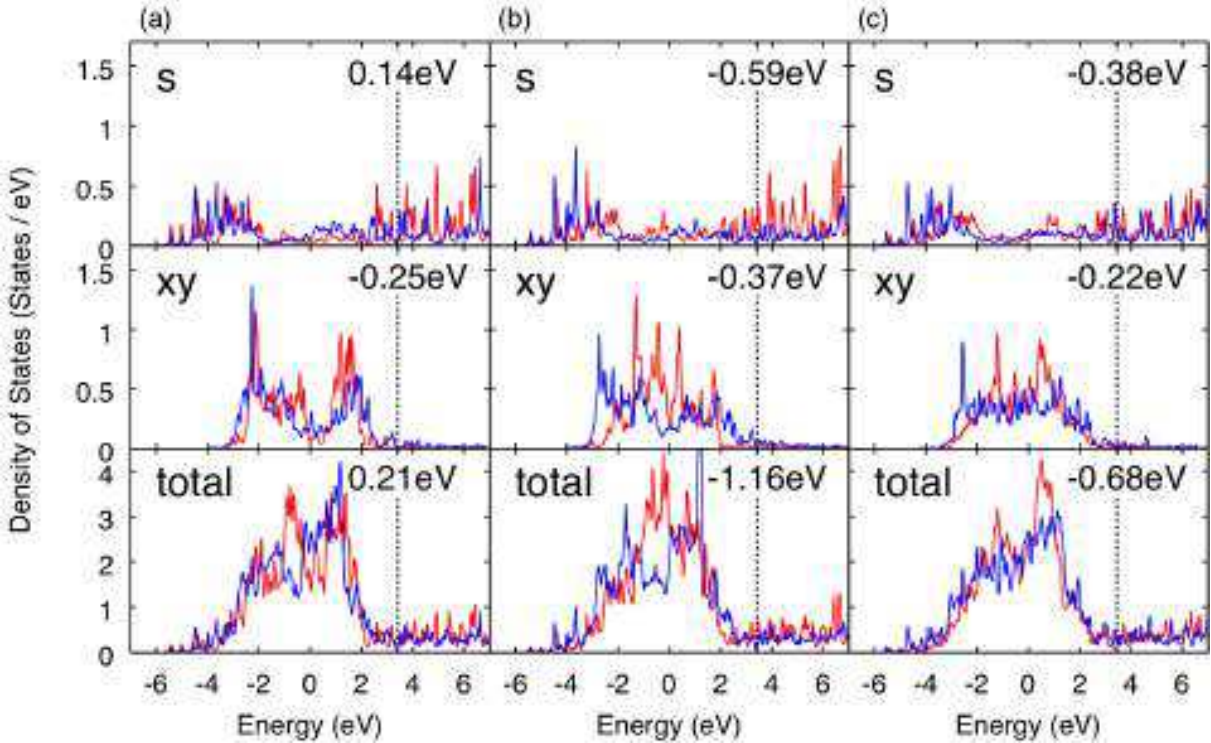


Figure 4: Partial densities of states and local energies of (a) the atom A, (b) the Atom C, and (c) the atom B. Red and blue lines are at initial state and at 500 MD step respectively in (a) and (b), and at 500 and 5,000 MD step in (c). Upper, middle, and lower figures are the partial densities of states of s -orbital, xy -orbital, and total density of states respectively. The energy changes of the densities of states are written at the upper right part of each figure. Notice that, in all cases, the asymmetry of the local density of state of xy orbital is enhanced.

loss of the atom A and the energy gain of the d -orbitals of atoms on the outermost shell. The change in the energy of d -orbitals is attributed to the enhancement of the asymmetry of LDOS originating from the development of flattened (111) faces and its gain/loss is almost proportional to the d -band width.

The change of LDOS of the atom B, on the edge of the (111) and (001) faces, in Stage 2 is depicted in Fig. 4 (c) by using the local coordinate system that x axis is the nanowire axis [110] and y axis is lateral [1 $\bar{1}$ 0]. The local energy of the s -orbital decreases since the coordination number of the atom B increases from seven to eight (Fig. 4 (c) top). The local energy in the

xy -orbital also decreases since the face transforms to (111) and is flattened (Fig. 4 (c) middle). Here, the slip deformation is essentially important since it widens the area of the (111) triangular face and the local density of the xy -orbital transfers its weight from the anti-bonding region to the bonding region. Therefore, both orbital effects result in the decrease of the local energy of the atom B. Since the neighboring atom A is now dissociated from the inner shell and can move easily, the atom B slips easily on the wire surface without dissociating their bonds and the helical structure appears.

The two-stage formation model holds in 12-6-1 and 13-6-1 nanowires. Figures 2(c)(d) show how inserted atom row would behave. See supplementary video. Both nanowires show surface reconstruction, and the number of atoms in the outermost shell is 13. Then the inserted atoms are supplied possibly from outer and inner shells and the surface reconstruction is not sensitive on positions of supplied atoms.

In all cases, the bond dissociation between the outermost atoms and the inner shell starts near a cross edge of two ideal faces, since the energy gain is maximized by flattening a surface on the edges. The ratio of the energy gain to the total energy due to the dissociation becomes smaller in thicker nanowires and then the thicker nanowires do not transform.

MD simulation for 11-4 and 12-6-1 nanowires in copper does not show the bond dissociations from the inner shell of Stage 1 at 600K within 500 MD steps, since copper has narrower d -band width. At 900 K the atom row slips on the (001) face in copper nanowires, since the atom have dissociated from the inner shell at that temperature.

The present analysis shows that the mechanism in both Stage 1 and Stage 2 is governed by the d -band width and the helical nanowires appear only among metals with a wider d -band. The d -band width in platinum and gold is commonly wider than that in lighter element, Ag and Cu, and the present theory explains why platinum nanowire can be also formed with helicity. The present mechanism is concerned not only with nanowires but also with the bulk surface, e.g. the

Au(001) surface reconstruction to Au(001)-hex, hexagonal close-packed one. (13, 14)

References

1. Y. Kondo, K. Takayanagi, *Science* **289**, 606 (2000).
2. Y. Oshima, A. Onga, K. Takayanagi, *Phys. Rev. Lett.* **91**, 205503 (2003).
3. Y. Oshima, *et al.*, *Phys. Rev. B* **65**, 121401 (2002).
4. O. Gülsen, F. Ercolessi, E. Tosatti, *Phys. Rev. Lett.* **80**, 3775 (1998).
5. B. Wang, S. Yin, G. Wang, A. Buldum, J. Zhao, *Phys. Rev. Lett.* **86**, 2046 (2001).
6. G. Bilalbegović, *Vacuum* **71**, 165 (2003).
7. E. Tosatti, S. Prestipino, S. Kostlmeier, A. Dal Corso, F. D. Di Tolla, *Science* **291**, 288 (2001).
8. R. T. Senger, S. Dag, S. Ciraci, *Phys. Rev. Lett.* **93**, 196807 (2004).
9. M. J. Mehl, D. A. Papaconstantopoulos, *Phys. Rev. B* **54**, 4519 (1996).
10. F. Kirchhoff, M. J. Mehl, N. I. Papanicolaou, D. A. Papaconstantopoulos, F. S. Khan, *Phys. Rev. B* **63**, 195101 (2001).
11. E. Z. da Silva, A. J. R. da Silva, A. Fazzio, *Phys. Rev. Lett.* **87**, 256102 (2001).
12. E. Z. da Silva, F. D. Novaes, A. J. R. da Silva, A. Fazzio, *Phys. Rev. Lett.* **69**, 115411 (2004).
13. G. Binnig, H. Rohrer, C. Gerber, E. Stall, *Surf. Sci.* **144**, 321 (1984).
14. N. Takeuchi, C. T. Chan, K. M. Ho, *Phys. Rev. B* **43**, 14363 (1991).